Inorganic Chemistry

Article

pubs.acs.org/IC

# Pyrazine-Based Organometallic Complex: Synthesis, Characterization, and Supramolecular Chemistry

Sourav Bhowmick,[†] Sourav Chakraborty,[†] Atanu Das,[‡] P. R. Rajamohanan,[§] and Neeladri Das*[,†]

[†]Department of Chemistry, Indian Institute of Technology Patna, Patna 800 013, Bihar, India

[‡]Department of Chemistry, University of Texas at Austin, Austin, Texas 78712, United States

[§]Central NMR Facility, CSIR National Chemical Laboratory, Dr. Homi Bhabha Road, Pune 411008, India

Supporting Information

**ABSTRACT:** The design, synthesis, and characterization of a new pyrazine-based ditopic platinum(II) organometallic complex are reported. The molecular structure of the organoplatinum pyrazine dipod was determined by single-crystal X-ray crystallography. The potential utility of this organometallic ditopic acceptor as a building block in the construction of neutral metallasupramolecular macrocycles containing the pyrazine motif was explored. Pyrazine motifs containing supramolecules were characterized by multinuclear NMR (including $^1$H DOSY), mass spectrometry, and elemental analysis. The geometry of each supramolecular framework was optimized by employing the PM6 semi-empirical molecular orbital method to predict its shape and size. The ability of the pyrazine-based organoplatinum complex to act as a host for nitroaromatic guest (2,4-dinitrotoluene and PA) molecules was explored by isothermal titration calorimetry (ITC). The binding stoichiometry and thermodynamic parameters of these host–guest complexation reactions were evaluated using ITC. Theoretical calculations were performed to obtain insight into the binding pattern between the organometallic host and nitroaromatic guests. The preferable binding propensity of the binding sites of complex **1** for both nitroaromatics (PA and 2,4-dinitrotoluene) determined by molecular simulation studies corroborates well with the experimental results as obtained by ITC experiments.

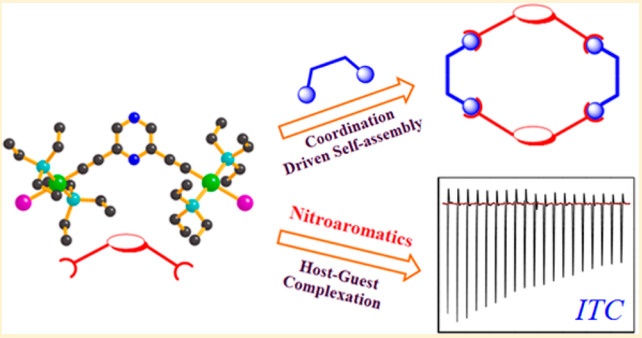


## INTRODUCTION

The design and self-assembly of finite supramolecular ensembles via a coordination-driven approach is an active field of research in contemporary supramolecular chemistry.[1] One of the prerequisites in the design of a new finite supramolecular framework is the synthesis of a new building block, which may also be referred to as a supramolecular synthon. In this context, several supramolecular synthons with interesting structural units [such as ferrocene, carboranes, cavitands, highly aromatic systems (such as anthracene, phenanthrene, perylene, pyrene, etc.), dendrons, and others] have been developed and subsequently used as tectons in the self-assembly of finite supramolecular ensembles such as metallacycles and metallacages.[1a,b,2] The incorporation of special structural motifs has been further exploited in terms of the use of supramolecular frameworks as catalysts,[3] molecular sensors,[4] molecular flasks,[5] molecular devices,[6] and hosts in host–guest chemistry.[7]

In the realm of the coordination-driven self-assembly of supramolecules, organometallic complexes based on square-planar platinum(II) centers have emerged as popular target molecules in the design of new metal-containing "acceptor" subunits. Depending on the nature (neutral or ionic) of the complementary "donor" linker, the resulting self-assembled ensemble is either charged or neutral. As far as the synthesis of neutral finite self-assemblies is concerned, a well-accepted strategy is to use anionic bridging linkers (as donors) in association with complementary cationic metal-containing subunits (as acceptors).[1a,b]

In more recent times, there has been a lot of research interest in the design of new platinum(II)-based organometallic complexes containing ethynyl spacer groups.[8] This is because of their use in the construction of ensembles with potential application in sensing nitroaromatics (DNT = 2,4-dinitrotoluene, TNT = 1,3,5-trinitrotoluene, and PA = picric acid).[4a,9] It is believed that the presence of platinum ethynyl motifs as well as a conjugated $\pi$-electron backbone is responsible for the efficient detection of trace nitroaromatic explosive materials.[9]

In a continuation of our research interest to develop new organometallic linkers and explore their potential applications as synthons in supramolecular self-assembly and host–guest chemistry,[10] herein we report the synthesis and characterization of a unique ditopic pyrazine-based organoplatinum complex (**1**) containing the platinum ethynyl motifs. Organoplatinum complex **1** has been fully characterized by several spectroscopic

**Received:** October 25, 2014
**Published:** February 26, 2015





DOI: 10.1021/ic502581x
*Inorg. Chem.* 2015, 54, 2543–2550

**Scheme 1. Synthesis of Pyrazine-Based Organoplatinum Complex 1**

techniques, and its structure has been determined by single-crystal X-ray diffraction. This new organoplatinum complex is structurally rigid with predefined binding angles and therefore is well-suited to act as a metal-containing acceptor supramolecular synthon for use in coordination-driven self-assembly protocols. To illustrate this point, three new platinum(II)-based neutral and nanoscalar supramolecular macrocycles (**2**−**4**) have been self-assembled using this pyrazine-based organometallic ditopic linker (**1**) as the acceptor unit and various dicarboxylates as bridging donor ligands. Supramolecules **2**−**4** are unique examples of neutral macrocycles that are self-assembled from a pyrazine-based organometallic tecton. In other words, the use of a pyrazine-based organometallic complex in the construction of metallamacrocycles has not been reported to date. These newly synthesized macrocycles (**2**−**4**) were completely characterized by multinuclear NMR spectroscopy including $^{1}$H DOSY NMR, mass spectrometry (MALDI-TOF-MS), and elemental analysis.

The pyrazine-containing organometallic complex **1** contains platinum ethynyl motifs in its backbone. Hence, the ability of complex **1** to act as the host for nitroaromatic guest molecules was explored. Using isothermal titration calorimetry (ITC) as a tool, it has been shown that **1** can efficiently form host−guest complexes with DNT and PA with high binding affinities. ITC has thus been used to evaluate the thermodynamic parameters of these host−guest complexation reactions. Computational studies corroborate with the experimental results as obtained from ITC experiments.

## RESULTS AND DISCUSSION

**Synthesis and Characterization of the Organometallic Acceptor Linker 1.** There are several reports in the literature wherein transition-metal-bearing $\sigma$-bonded acetylene motifs have been designed for subsequent use in supramolecular chemistry.[8] In this context, it must be mentioned that organometallic complexes containing platinum ethynyl motifs can be conveniently prepared by the reaction of *trans*-$PtI_2(PEt_3)_2$ with organic molecules containing multiple ethynyl functional groups.[8,9] Inspired by these reports, the pyrazine-based organometallic complex **1** was efficiently synthesized by reacting 2,6-diethynylpyrazine with 2 equiv of *trans*- $PtI_2(PEt_3)_2$ in the presence of CuI (catalyst), triethylamine (base), and toluene (solvent) at room temperature for 16 h (Scheme 1). This pyrazine-based organometallic complex, obtained as a white solid, is stable in air/moisture and has high solubility in common organic solvents. This diiodo organometallic complex (**1**) has been fully characterized by Fourier transform infrared (FTIR), multinuclear NMR ($^{1}$H and $^{31}$P) spectroscopy, single-crystal X-ray crystallography and elemental analysis. In the FTIR spectrum of **1**, the presence of an ethynyl functional group was evident because of the presence of an an intense peak at 2106 cm$^{-1}$. The $^{1}$H NMR spectrum of complex **1** recorded in $CDCl_3$ exhibits a sharp singlet at 8.16 ppm that corresponds to the aromatic protons of pyrazine. As expected, the methylene and methyl protons of the $PEt_3$ groups appear as multiplets between 1.13 and 2.26 ppm. The $^{31}$P NMR spectrum of **1** shows one sharp singlet at 8.87 ppm with accompanying $^{195}$Pt satellites ($^{1}J_{PPt}$ = 1147 Hz). The appearance of one sharp signal in $^{31}$P NMR suggests that all phosphorus nuclei attached to platinum(II) centers are chemically equivalent as well as have the overall symmetrical structure of complex **1**. The molecular structure of **1** was confirmed unambiguously by single-crystal X-ray crystallographic analysis.

**X-ray Crystallographic Analysis of 1.** Slow vapor diffusion of acetone into a dichloromethane solution of complex **1** at ambient temperature yielded single crystals suitable for X-ray crystallographic analysis. The ball-and-stick representation of the molecular structure of **1** is shown in Figure 1. Complex **1** crystallizes in monoclinic space group *C*2/*c*. Crystallographic analysis suggests that the platinum(II) centers display slightly distorted square-planar geometry with the cis angles (around the platinum centers) in the range 85−94°. The molecular structure also reveals that **1** is a 120° acceptor tecton because the Pt−pyrazine−Pt angle is 119.9°. The distance between two platinum centers is 10.29 Å. No unusual bond lengths and bond angles were observed in the structural analysis of **1**.

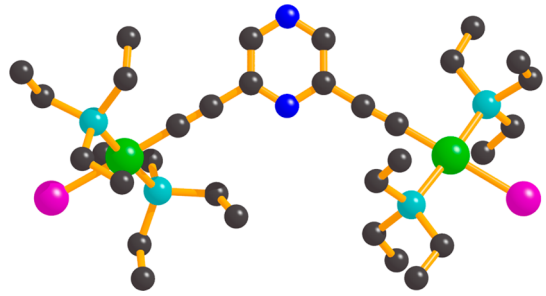

**Figure 1.** Molecular structure (ball-and-stick representation) of the pyrazine-based 120° $Pt^{II}_2$ organometallic complex **1** (green, Pt; violet, I; cyan, P; blue, N; black, C). Hydrogen atoms are omitted for the sake of clarity.

**Application of Complex 1 as a Molecular Tecton for the Self-Assembly of 2D Macrocycles.** The pyrazine-based $Pt^{II}_2$ complex **1** is a ditopic linker (having two reactive sites) and hence, can act as a potential acceptor linker. According to the "directional-bonding" approach,[1b,11] it is anticipated that the reaction of **1** with a suitable ditopic donor linker in an equimolar ratio would result in the self-assembly of two-dimensional (2D) macrocyclic architectures. In order to validate the above hypothesis, three different dicarboxylates were selected to react with the $Pt^{II}_2$ complex **1** separately. The iodine units (attached to the platinum center) of complex **1** were abstracted by a salt metathesis reaction with 2 equiv of $AgNO_3$ in acetone and subsequently reacted with an aqueous solution of the respective dicarboxylate donor ligand, $\mathbf{L_1}$−$\mathbf{L_3}$ [$\mathbf{L_1}$ = terephthalate, $\mathbf{L_2}$ = isophthalate, and $\mathbf{L_3}$ = fumarate] in a 1:1 stoichiometric ratio. This resulted in the gradual



DOI: 10.1021/ic502581x
*Inorg. Chem.* 2015, 54, 2543−2550

**Scheme 2. Self-Assembly of [2 + 2] Macrocycles 2−4 Using the Pyrazine-Based Organometallic $Pt^{II}_2$-Acceptor Tecton 1 and Dicarboxylate Donors $L_1$−$L_3$**

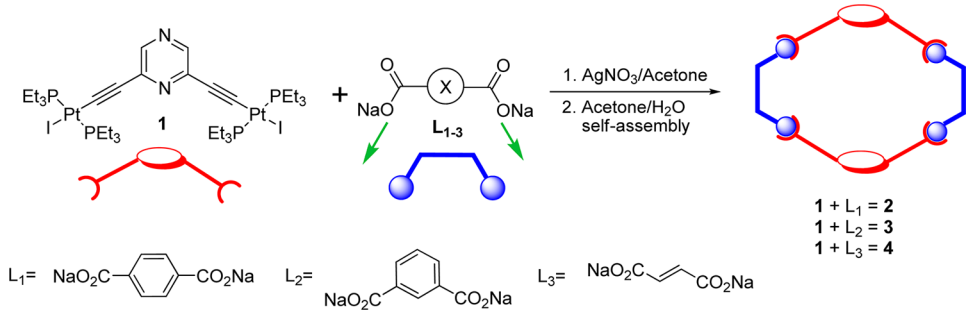


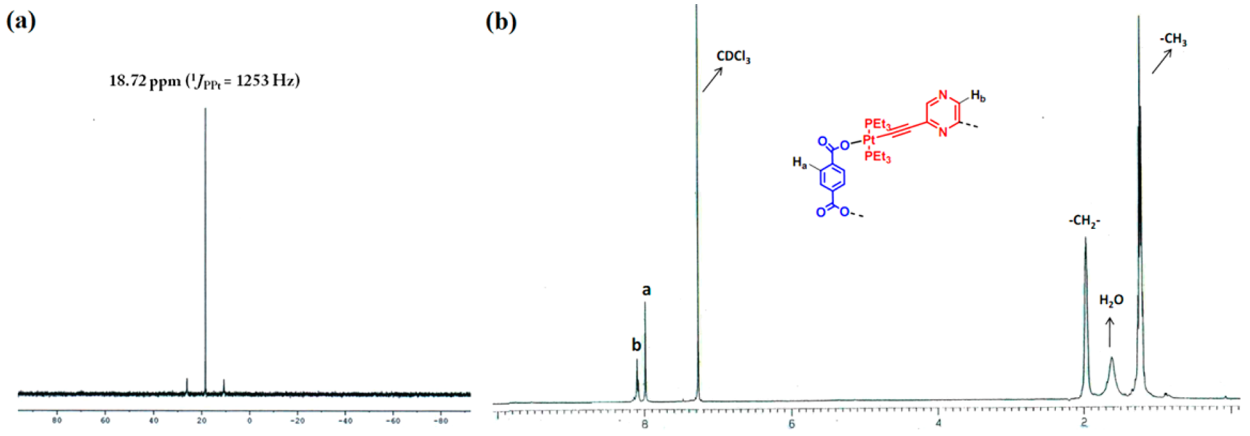


**Figure 2.** (a) $^{31}P\{^1H\}$ NMR and (b) $^1H$ NMR spectra of macrocycle **2** recorded in $CDCl_3$.

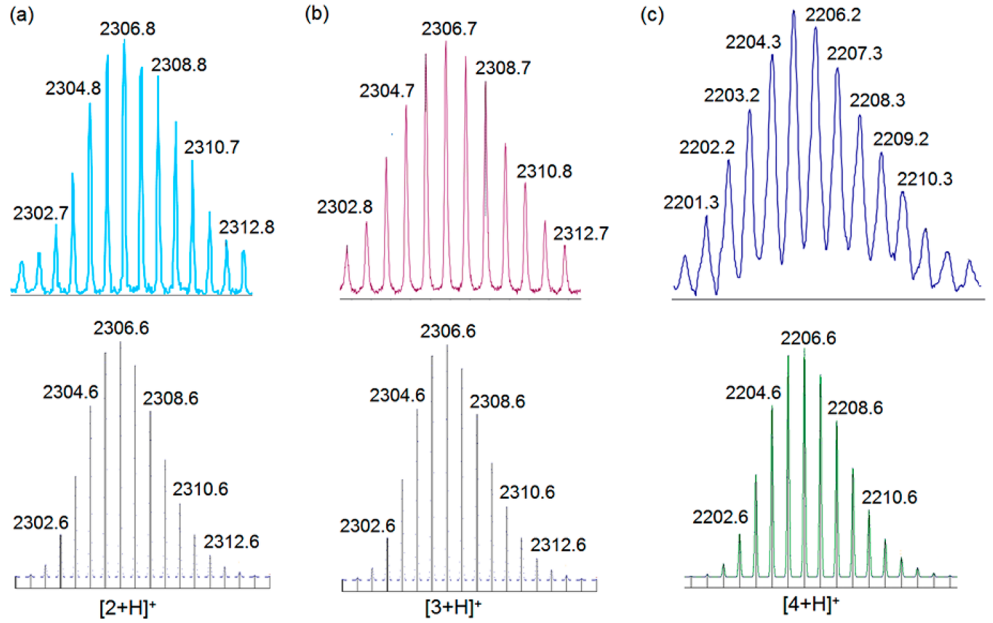


**Figure 3.** Experimental (top) and theoretical (bottom) MALDI-TOF-MS spectra of (a) macrocycles **2**, (b) **3**, and (c) **4**.

precipitation of the desired neutral self-assembled 2D macrocycles **2**−**4** as white solids (Scheme 2).

**Characterization of Self-Assembled Ensembles 2−4.** The products thus obtained in these self-assembled reactions were found to be soluble in common organic solvents including halogenated solvents such as chloroform or dichloromethane. These newly synthesized self-assembled ensembles were completely characterized by multinuclear NMR spectroscopy, MALDI-TOF-MS and elemental analysis. Initial evidence for the formation of discrete supramolecular species was obtained from NMR spectroscopic studies of compounds **2**−**4**. The presence of a sharp singlet peak (18.72 ppm for **2**, 18.84 ppm for **3**, and 18.71 ppm for **4**) in the respective $^{31}P\{^1H\}$ NMR spectrum along with a pair of accompanying platinum satellites



DOI: 10.1021/ic502581x
Inorg. Chem. 2015, 54, 2543−2550

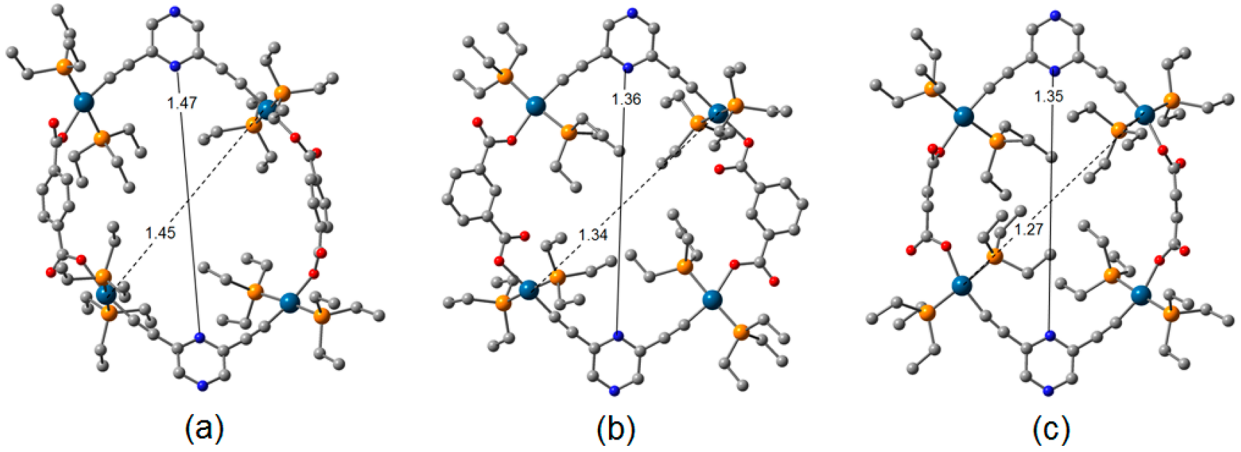


**Figure 4.** Simulated ball-and-stick molecular model of macrocycles (a) **2**, (b) **3**, and (c) **4** optimized by PM6 semiempirical molecular orbital methods (light gray, C; orange, P; dark cyan, Pt; blue, N). Hydrogen atoms are omitted for clarity.

($^1J_{PPt}$ = 1253 Hz for **2**, $^1J_{PPt}$ = 1246 Hz for **3**, and $^1J_{PPt}$ = 1234 Hz for **4**) clearly suggested the formation of a highly symmetrical supramolecular framework in which all of the phosphorus nuclei are equivalent (Figure 2 and Supporting Information, SI). It must be mentioned here that the significant downfield shifts observed in the phosphorus signals of compounds **2**−**4** suggested cleavage of the Pt−I bond, thereby leading to the formation of a new metal−ligand coordination reaction at the platinum centers.

The $^1$H NMR spectra of **2**−**4** clearly suggested the incorporation of both the respective dicarboxylate and the pyrazine motif in the final products. A representative $^1$H NMR spectrum of **2** is shown in Figure 2. The signal at 8.07 ppm corresponds to the protons of the pyrazine moiety, whereas the sharp singlet at 7.97 ppm is due to the aromatic protons of the terephthalate unit. Peaks in the range of 1.16−2.08 ppm are due to the ethyl protons of the $PEt_3$ group coordinated to the platinum(II) centers. Similarly, signals observed in the $^1$H NMR spectra of **3** and **4** were assigned precisely (see the SI). In the case of all three compounds **2**−**4**, the integration ratio of peaks due to the dicarboxylate moiety and pyrazine-based $Pt^{II}_2$ units suggested a self-assembly reaction in a 1:1 stoichiometric ratio.

Additional information on the purity of the metallamacrocycles **2**−**4** was obtained from $^1$H DOSY NMR spectroscopy in the case of each compound. These organometallic macrocycles advocate a single trace in the DOSY NMR (see the SI), indicating the formation of a single product and ruling out the presence of additional species such as other macrocycles or oligomers in solution.

Compounds **2**−**4** were subjected to mass spectrometric analysis (MALDI-TOF-MS) to confirm that the reaction of **1** with dicarboxylates $\mathbf{L_1}$−$\mathbf{L_3}$ indeed yielded [2 + 2] macrocycles in each case (Figure 3). The MALDI-TOF-MS spectrum of macrocycle **2** showed a strong peak at $m/z$ 2306.8 corresponding to the $[\mathbf{2} + H]^+$ charge state, thereby confirming the formation of a [2 + 2] self-assembled ensemble due to the reaction between two units each of pyrazine containing $Pt^{II}_2$ unit **1** and terephthalate moieties. Similarly, in the case of **3** and **4**, the formation of [2 + 2] self-assembled macrocycles was established by MALDI-TOF-MS analysis because of the presence of peaks at $m/z$ 2306.7and 2206.2 corresponding to the respective $[M + H]^+$ charge state (M corresponds to the molar mass of intact dimeric species **3** or **4**). These mass signals were isotopically resolved and the isotopic resolutions were found to be in good agreement with the corresponding theoretically predicted isotopic distribution assuming the formation of [2 + 2] macrocycles (Figure 3). Thus, mass spectrometric analysis unambiguously confirmed the formation of [2 + 2] neutral metallamacrocycles involving two units each of the pyrazine-based $Pt^{II}_2$ acceptor unit **1** and the respective dicarboxylate donor linker.

**PM6 Molecular Modeling of Self-Assembled Ensembles 2−4.** All attempts to grow single crystals (of **2**−**4**) for structural characterization have been unsuccessful to date. Nevertheless, in order to obtain useful information regarding the shape of differently sized voids present in these macrocycles, a PM6 semiempirical molecular orbital method[12] was employed to optimize their geometry. The energy-minimized structures of **2**−**4** suggest distorted oval-shaped internal cavities, as depicted in the perspective views (Figure 4). The optimized geometry of macrocycles **2**−**4** also reveals that in all cases the platinum centers display slightly distorted square-planar geometry. The distance between the two endocyclic nitrogen atoms of the pyrazine moieties was estimated to be 1.47, 1.36, and 1.35 nm for macrocycles **2**−**4**, respectively. The farthest distances between two diagonally opposite platinum centers in the case of macrocycles **2**−**4** were found to be 1.45, 1.34, and 1.27 nm, respectively.

**Study of Host−Guest Complexation between 1 and Nitroaromatics Using ITC.** After establishing the potential use of **1** as a metal-containing acceptor tecton in coordination-driven self-assembly reactions, we were interested in exploring the host−guest binding interaction of this organometallic complex **1** with nitroaromatics such as PA and DNT. It must be mentioned here that PA and DNT are relatively electron-deficient species because of the presence of strong electron-withdrawing nitro groups in their respective aromatic rings. On the other hand, the presence of ethynyl motifs in conjugation with the pyrazine core renders **1** a $\pi$-electron-rich species relative to DNT or PA.[9]

Unfortunately, complex **1** was found to be nonfluorescent in nature, and therefore the study of host−guest complexation between **1** and nitroaromatics using fluorescence spectroscopy was not a viable option. In such a scenario, the ITC technique was utilized to study the aforementioned host−guest chemistry.

In supramolecular chemistry, ITC has been used as a useful analytical tool to study host−guest interactions. Using ITC, the


DOI: 10.1021/ic502581x
*Inorg. Chem.* 2015, 54, 2543−2550

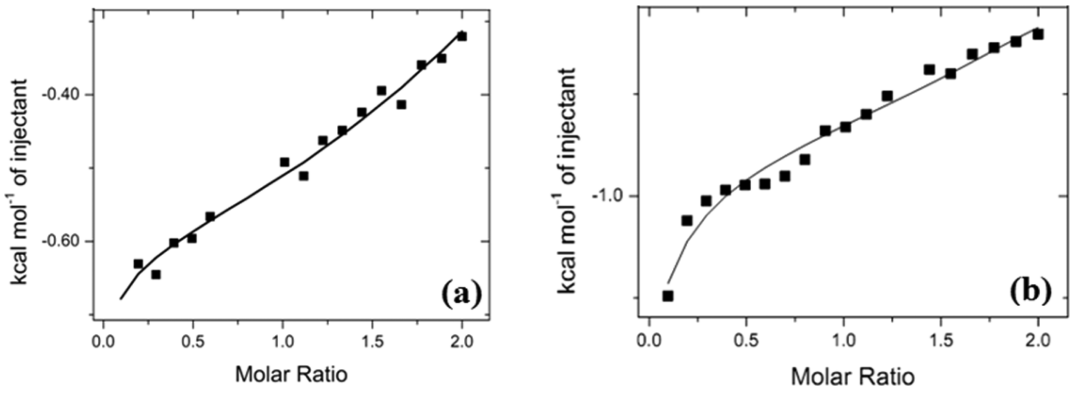


**Figure 5.** (a) ITC data points best fitted with two sets of site models for the titration of **1** (4 mM) into PA (0.4 mM) at 298 K in methanol. (b) ITC data points best fitted with a sequential two-site binding model for the titration of **1** (5 mM) into DNT (0.5 mM) at 298 K in methanol.

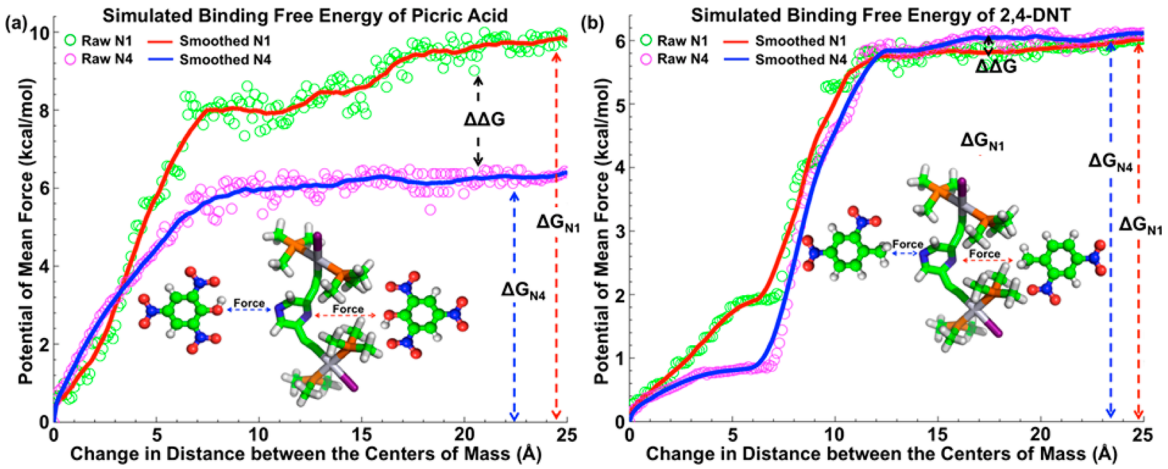


**Figure 6.** Binding free-energy estimation from WHAM. Comparison of PMF profiles as a function of the distance pulled for the two separate binding sites (N1 and N4) of complex **1** with (a) PA and (b) DNT. Inset images are intended to depict the directions of the pulling pathways for the two potential binding sites of the pyrazine-based organoplatinum complex. Complex **1** is shown as a licorice representation. The nitroaromatic compounds PA and DNT are shown in ball and stick.

thermodynamic parameters of binding interactions between the host and guest can be accurately estimated and the data may be further utilized to calculate the respective binding constant value.

In the case of host–guest complexation between **1** and PA, the ITC trace recorded at 25 °C suggests that the binding interactions are exothermic in nature. The ITC data were found to fit with a two-site sequential binding model (Figure 5a). The data did not fit satisfactorily with other models. This clearly indicates that the pyrazine complex **1** and PA form a 1:2 host–guest complex. The thermodynamic parameters obtained from the ITC data are tabulated in Table S1 in the SI. From the ITC data, the binding constant values were obtained as $K_1 = 2.7 \times 10^3\ M^{-1}$ and $K_2 = 2.2 \times 10^4\ M^{-1}$.

In the case of binding between the organometallic linker **1** and DNT, the titration data points fitted best with a two-site sequential binding model (Figure 5b). The binding data confirm the formation of a 1:2 host–guest complex between **1** and DNT with the binding constants $K_1 = 2.0 \times 10^4\ M^{-1}$ and $K_2 = 2.6 \times 10^4\ M^{-1}$.

The ITC data clearly suggest that, in the case of PA as the guest, one of the two binding sites in **1** has higher binding affinity than the other site. However, in the other case, both binding sites in complex **1** have comparable binding affinity for DNT guest moieties. Additionally, the magnitude of the binding constants obtained suggests that pyrazine-based organometallic complex **1** has a reasonably high binding affinity for both PA and DNT, which are chemical constituents of nitroaromatic explosives.

**Theoretical Calculation.** In the case of the organometallic linker **1** having a central pyrazine moiety, the nitroaromatics (PA and DNT) studied herein bind to both the N1 and N4 atoms of pyrazine, leading to the formation of **1**$(PA)_2$ and **1**$(DNT)_2$ complexes. In order to predict the primary (first binding) and secondary (second binding) sites among the two nitrogen centers (N1 and N4), computational studies were performed. It is evident from the ITC measurements that the pyrazine-based organoplatinum complex **1** has two binding sites, N1 and N4. To perform a comparative analysis of the binding affinities of the two nitroaromatic compounds PA and DNT toward the two binding sites of complex **1**, simulations were carried out with two different orientations of the nitroaromatic compounds (PA or DNT) with respect to complex **1**. Two initially bound state conformations of complex **1** with PA were generated by placing PA in close vicinity to complex **1** in two different orientations, one near the N1 atom and the other near the N4 atom. The same technique was followed for generation of the initially bound state conformations of complex **1** with DNT. The criterion for placing the nitroaromatic compounds near the N1 and N4


DOI: 10.1021/ic502581x
*Inorg. Chem.* 2015, 54, 2543–2550

atoms of complex **1** was such that no atoms of the nitroaromatic compounds were within the bonding radius of either the N1 or N4 atom of complex **1**. Thus, four initially bound states were generated and these structures equilibrated before the free energy of separation was measured in each case. The simulated result shows that PA has a preference for N1 over N4 (Figure 6a). The scenario gets reversed for DNT, which prefers to bind N4 over N1 (Figure 6b). However, the preference is much more prominent for PA because the difference in the binding free-energy values between N1 and N4 is ∼3.4 kcal $mol^{-1}$. The same difference is very nominal for DNT (∼0.1 kcal $mol^{-1}$). So, both nitrogen atoms of the pyrazine complex behave as competing binding sites for DNT.

Thus, the preferential binding sites in complex **1** as obtained from "pulling simulations" toward interaction with both the nitroaromatics PA and DNT were found to be in line with the conclusions drawn from ITC experiments.

## CONCLUSION

In conclusion, we describe herein the synthesis of a new organometallic complex containing two platinum(II) ethynyl units attached to the pyrazine ring at the C2 and C6 positions. Complex **1** is stable in air/moisture and has been characterized by FTIR, multinuclear NMR spectroscopy, mass spectrometry, and elemental analysis. Single-crystal X-ray diffraction analysis confirms that **1** is a 120° bent but structurally rigid bifunctional platinum(II)-based tecton. The divergent spatial orientation of the two platinum(II) centers with respect to each other renders **1** a potential acceptor building block in coordination-driven self-assembly for the synthesis of finite supramolecular frameworks. To illustrate this point, **1** was used as a supramolecular synthon along with complementary dicarboxylate donor linkers to yield neutral metallamacrocycles **2**−**4**. In this report, for the first time, we describe the use of a pyrazine-based organometallic complex in the design of supramolecular metallamacrocycles. NMR spectroscopy, including $^1$H DOSY NMR, of these metallamacrocycles (**2**−**4**) suggested the formation of highly symmetrical discrete moieties, thereby ruling out the formation of oligomeric species (thereby suggesting the formation of highly symmetrical discrete moieties). On the other hand, MALDI-TOF-MS and elemental analysis confirmed their respective composition and purity. Structural insights for the metallamacrocycles **2**−**4** were obtained from molecular simulations of the macrocycles using PM6 semiempirical molecular orbital methods. In addition to the use of **1** as a building block in coordination-driven supramolecular chemistry, its ability to act as a host for relatively electron-poor nitroaromatics was also tested using ITC. Our ITC studies suggest the formation of 1:2 host−guest species between **1** and PA/DNT. Theoretical calculations were performed to obtain information regarding primary (first binding) and secondary (second binding) sites on **1** to which the nitroaromatics get bound. Simulated binding free-energy estimations suggest altered behaviors of N1 and N4 of complex **1** toward binding of the two nitroaromatic compounds: preferable binding propensities of PA at N1 over N4 and comparable binding propensities of DNT at N1 and N4. Molecular simulation studies corroborate well with the experimental results obtained from ITC experiments. The pyrazine core containing organometallic supramolecular synthons, as described in this manuscript, has immense potential in the design of new supramolecular frameworks with anticipated applications in host−guest chemistry. Studies are currently underway in our laboratory in these directions.

## EXPERIMENTAL SECTION

**General Details.** All chemicals and anhydrous solvents used in this work were purchased from commercial sources and used without further purification. 2,6-Diethynylpyrazine[13] was prepared by following the reported literature procedures. FTIR spectra were recorded in a PerkinElmer Spectrum 400 FTIR spectrophotometer. $^1$H and $^{31}$P NMR spectra were recorded on Bruker 400 and 500 MHz spectrometers. Elemental analysis was carried out using a Thermo Scientific Flash 2000 organic elemental analyzer. MALDI-TOF-MS spectra of the compounds were recorded using a Bruker UltrafleXtreme MALDI-TOF/TOF mass spectrometer. DOSY NMR measurements were performed on a Bruker AV 500 NMR spectrometer using a 5 mm gradient probe at 298 K. DOSY experiments were done with a standard Bruker pulse sequence (ledbpgp2s) with a longitudinal eddy current delay.

**Synthesis of Compound 1.** 2,6-Diethynylpyrazine (0.10 g, 0.78 mmol) and *trans*-diiodobis(triethylphosphine)platinum(II) (2.13 g, 3.12 mmol) were charged in a 100 mL Schlenk flask in the glovebox. Subsequently, 40 mL of dry toluene and 5 mL of freshly distilled triethylamine were added under nitrogen. The solution was stirred for 10 min at room temperature before CuI (22 mg, 0.11 mmol) was added in one portion. After overnight stirring at room temperature, triethylammonium iodide precipitated from solution, which was separated by filtration. Toluene was evaporated in a rotary evaporator and the resulting yellow residue was purified by column chromatography on silica gel, eluting with 1% ethyl acetate in hexane first and then gradually increasing to 3% ethyl acetate in hexane to isolate complex **1** as a white solid.

Yield: 0.67 g, 70%. Mp: 148−150 °C. $^1$H NMR (500 MHz, $CDCl_3$): $\delta$ 8.16 (s, 2H, Ar−H), 2.21−2.26 (m, 24H, $-CH_2$), 1.13−1.19 (m, 36H, $-CH_3$). $^{31}$P NMR (202.5 MHz, $CDCl_3$): $\delta$ 8.87 ($^1J_{PPt}$ = 1147 Hz). IR (ATR): 2957, 2920, 2866, 2106, 1489, 1389, 1227, 1145, 1027, 753 $cm^{-1}$. Anal. Calcd for $C_{32}H_{62}I_2N_2P_4Pt_2$: C, 30.93; H, 5.03; N, 2.25. Found: C, 31.01; H, 5.09; N, 2.31.

**General Procedure for the Synthesis of Macrocycles 2−4.** To the solution of compound **1** (30 mg, 0.024 mmol) in acetone (5 mL) was added $AgNO_3$ (9 mg, 0.048 mmol) in one portion, and the reaction mixture was stirred for 4 h in the dark at room temperature. The precipitated AgI was filtered off over a bed of Celite, and the filtrate was collected. An aqueous solution (0.5 mL) of the respective dicarboxylate (0.024 mmol) was added dropwise to the filtrate with continuous stirring. The reaction mixture was stirred overnight at room temperature, and solvents were removed under reduced pressure to obtain a white solid, which was washed several times with water and subsequently dried in vacuum. This product was recrystallized from chloroform to obtain the desired macrocycles as a white microcrystalline solid.

*Macrocycle* ***2***. Yield: 26 mg, 84%. $^1$H NMR (400 MHz, $CDCl_3$): $\delta$ 8.07 (s, 4H, Ar−H), 7.97 (s, 8H, Ar−H), 2.06−2.08 (m, 48H, $-CH_2$), 1.16−1.24 (m, 72H, $-CH_3$). $^{31}$P NMR (163 MHz, $CDCl_3$): $\delta$ 18.72 ($^1J_{PPt}$ = 1253 Hz). IR (ATR): 2979, 2937, 2885, 2114, 1635, 1500, 1333, 1239, 1157, 1031, 740 $cm^{-1}$. Anal. Calcd for $C_{80}H_{132}N_4O_8P_8Pt_4$: C, 41.67; H, 5.77; N, 2.43. Found: C, 41.74; H, 5.83; N, 2.51. MALDI-TOF-MS. Calcd for $[M + H]^+$: *m*/*z* 2306.6. Found: *m*/*z* 2306.8.

*Macrocycle* ***3***. Yield: 27 mg, 87%. $^1$H NMR (500 MHz, $CDCl_3$): $\delta$ 8.59 (s, 4H, Ar−H), 8.12 (s, 2H, Ar−H), 8.05−8.08 (m, 4H, Ar−H), 7.34−7.37 (m, 2H, Ar−H), 1.95−1.96 (m, 48H, $-CH_2$), 1.13−1.24 (m, 72H, $-CH_3$). $^{31}$P NMR (202.5 MHz, $CDCl_3$): $\delta$ 18.84 ($^1J_{PPt}$ = 1246 Hz). IR (ATR): 2985, 2957, 2895, 2125, 1646, 1512, 1344, 1245, 1230, 1042, 730 $cm^{-1}$. Anal. Calcd for $C_{80}H_{132}N_4O_8P_8Pt_4$: C, 41.67; H, 5.77; N, 2.43. Found: C, 41.70; H, 5.73; N, 2.48. MALDI-TOF-MS. Calcd for $[M + H]^+$: *m*/*z* 2306.6. Found: *m*/*z* 2306.7.

*Macrocycle* ***4***. Yield: 25 mg, 83%. $^1$H NMR (500 MHz, $CDCl_3$): $\delta$ 8.07 (s, 4H, Ar−H), 6.65 (s, 4H, −CH), 1.91−1.97 (m, 48H, $-CH_2$), 1.16−1.20 (m, 72H, $-CH_3$). $^{31}$P NMR (202.5 MHz, $CDCl_3$): $\delta$ 18.71 ($^1J_{PPt}$ = 1234 Hz). IR (ATR): 2979, 2927, 2875, 2104, 1615, 1489,


DOI: 10.1021/ic502581x
*Inorg. Chem.* 2015, 54, 2543−2550

1323, 1230, 1146, 1031, 740 $cm^{-1}$. Anal. Calcd for $C_{72}H_{128}N_4O_8P_8Pt_4$: C, 39.20; H, 5.85; N, 2.54. Found: C, 39.26; H, 5.92; N, 2.60. MALDI-TOF-MS: Calcd for $[M + H]^+$: $m/z$ 2206.6. Found: $m/z$ 2206.2.

**Crystallographic Data Collection and Refinement.** The single crystal of compound **1** was mounted on the tip of a glass fiber with commercially available glue. Single-crystal X-ray data collection of **1** was performed at 298 K using a Bruker APEX II diffractometer, equipped with a normal-focus, sealed-tube X-ray source with graphite-monochromated Mo K$\alpha$ radiation ($\lambda$ = 0.71073 Å). The data were integrated using the *SAINT*[14] program, and the absorption corrections were made with *SADABS*.[15] The structure of **1** was solved by *SHELXS-97*[16] using the Patterson method, followed by successive Fourier and difference Fourier synthesis. Full-matrix least-squares refinements were performed on $F^2$ using *SHELXL-97*[16] with anisotropic displacement parameters for all non-hydrogen atoms. All of the hydrogen atoms were fixed geometrically by the *HFIX* command and placed in ideal positions. Calculations were carried out using *SHELXS-97*,[16] *SHELXL-97*,[16] *PLATON*, version 1.15,[17] *ORTEP-3v2*,[18] and *WinGX* system, version 1.80.[19] Data collection and structure refinement parameters along with crystallographic data of **1** are given below.

*Crystal Data of* ***1****:* $C_{32}H_{62}I_2N_2P_4Pt_2$, $M$ = 1242.68, monoclinic, space group $C2/c$, $a$ = 40.263(4) Å, $b$ = 9.4403(8) Å, $c$ = 23.128(2) Å, $\beta$ = 108.01 (3)°, $V$ = 8359.9(13) $Å^3$, $T$ = 298 K, $Z$ = 8, $D_{calc}$ = 1.975 g $cm^{-3}$, $\mu$ = 8.339 $mm^{-1}$, 46668 reflections measured, 10444 unique ($R_{int}$ = 0.069), R1 [$I > 2\sigma(I)$] = 0.0344, wR2 ($F$, all data) = 0.1031, GOF($F^2$) = 1.16. CCDC 1028296.

**ITC To Study the Thermodynamics of Host−Guest Chemistry of 1 and Nitroaromatics.** ITC experiments were performed on a MicroCal-iTC200 calorimeter (GE Healthcare Life Science) at 25 °C. All experiments were done using methanol as the solvent. Each experiment was done with 20 consecutive injections (2 $\mu$L) of complex **1** (solution in methanol, 4 mM PA, and 5 mM DNT) into a methanol solution of nitroaromatics (280 $\mu$L, 0.4 mM PA, and 0.5 mM DNT) with 2 min intervals between successive injections. The rotation speed of the syringe was maintained at 600 rpm. The integration of the heat pulses obtained from each titration was fitted using *MicroCal Origin 7.0* software to determine the site-binding model and to obtain the enthalpy change ($\Delta H$), entropy change ($\Delta S$), and corresponding association constant ($K$).

**Simulation Protocol.** Complex **1** bound to PA and DNT was used for umbrella sampling[20] and weighted histogram analysis method (WHAM)[21] assays to measure the binding free energies of the nitroaromatic compounds at both N1 and N4 of complex **1**, separately. Conformations for umbrella sampling were obtained after 100 ns of equilibration, using steered molecular dynamics simulations[22] (tether speed 0.001 nm $ps^{-1}$) in simple point charge explicit solvent[23] using *CHARMM27* force-field parameters.[24] The *LINCS* algorithm was applied to constrain all bond lengths that contained a hydrogen atom.[25] All of the simulations were conducted using the *GROMACS* software package,[26] version 4.5.5. A full description of the methods is given in the SI.

## ■ ASSOCIATED CONTENT

### Supporting Information

$^1H$ and $^{31}P\{^1H\}$ NMR spectra for complexes **1** and metallacycles **2**−**4**, $^1H$ DOSY NMR spectra of the metallacycles, ITC isotherm data and thermodynamic parameters for the binding of **1** to nitroaromatics as obtained by ITC, detailed simulation protocol. and X-ray crystallographic file (CIF) for **1**. This material is available free of charge via the Internet at http://pubs.acs.org. CCDC 1028296 also contains the supplementary crystallographic data for **1**. These data can be obtained free of charge from The Cambridge Crystallographic Data Centre via www.ccdc.cam.ac.uk/data_request/cif.

## ■ AUTHOR INFORMATION


### Corresponding Author

*E-mail: neeladri@iitp.ac.in or neeladri2002@yahoo.co.in. Tel. +91 612 2552023. Fax +91 612 2277383.


### Author Contributions

N.D. concieved the research and supervised the work. S.B. synthesized all compounds (**1**−**4**) reported in this manuscript. S.C. performed the ITC experiments and also optimized the energy-minimized geometry of the metallacycles **2**−**4**. P.R.R. recorded the DOSY NMR spectra of the metallacycles **2**−**4**. A.D. carried out the theoretical calculations to study host−guest complexation between complex **1** and nitroaromatics and also optimized the binding free-energy values from "pulling simulations". S.C., A.D., and N.D. wrote and all authors edited the manuscript.

### Notes

The authors declare no competing financial interest.

## ■ ACKNOWLEDGMENTS


N.D. thanks the Indian Institute of Technology (IIT) Patna for financial support. S.C. and S.B. thank IIT Patna for an Institute Research Fellowship. The authors also acknowledge Dr. Sivaramaiah Nallapeta (Bruker Daltonics India) for MALDI-TOF mass spectrometric data. Prof. Dmitrii E. Makarov is acknowledged for allowing A.D. to use the computational resources at the University of Texas at Austin provided by the Texas Advanced Computing Center. A.D. acknowledges funding from Robert A. Welch foundation (Grant No. F-1514). The authors also acknowledge SAIF-Panjab University and SID, IISc Bangalore for providing analytical facilities.


## ■ REFERENCES


(1) (a) Cook, T. R.; Zheng, Y.-R.; Stang, P. J. *Chem. Rev.* **2013**, *113*, 734. (b) Chakrabarty, R.; Mukherjee, P. S.; Stang, P. J. *Chem. Rev.* **2011**, *111*, 6810. (c) Pluth, M. D.; Bergman, R. G.; Raymond, K. N. *Acc. Chem. Res.* **2009**, *42*, 1650. (d) Yoshizawa, M.; Fujita, M. *Bull. Chem. Soc. Jpn.* **2010**, *83*, 609. (e) Yoshizawa, M.; Klosterman, J. K.; Fujita, M. *Angew. Chem., Int. Ed.* **2009**, *48*, 3418. (f) Oliveri, C. G.; Ulmann, P. A.; Wiester, M. J.; Mirkin, C. A. *Acc. Chem. Res.* **2008**, *41*, 1618. (g) Samanta, D.; Mukherjee, P. S. *Chem. Commun.* **2014**, *50*, 1595. (h) Young, N. J.; Hay, B. P. *Chem. Commun.* **2013**, *49*, 1354. (i) Thanasekaran, P.; Lee, C.-C.; Lu, K.-L. *Acc. Chem. Res.* **2012**, *45*, 1403. (j) Therrien, B. *Chem.—Eur. J.* **2013**, *19*, 8378. (k) Cook, T. R.; Vajpayee, V.; Lee, M. H.; Stang, P. J.; Chi, K.-W. *Acc. Chem. Res.* **2013**, *46*, 2464. (l) Clegga, J. K.; Li, F.; Lindoy, L. F. *Coord. Chem. Rev.* **2013**, *257*, 2536. (m) Saha, M. L.; Neogi, S.; Schmittel, M. *Dalton Trans.* **2014**, *43*, 3815. (n) Mishra, A.; Gupta, R. *Dalton Trans.* **2014**, *43*, 7668.

(2) (a) Northrop, B. H.; Yang, H.-B.; Stang, P. J. *Chem. Commun.* **2008**, 5896 and references cited therein. (b) Fujita, M.; Yu, S.-Y.; Kusukawa, T.; Funaki, H.; Ogura, K.; Yamaguchi, K. *Angew. Chem., Int. Ed.* **1998**, *37*, 2082. (c) Xu, L.; Chen, L.-J.; Yang, H.-B. *Chem. Commun.* **2014**, *50*, 5156 and references cited therein.

(3) (a) Pluth, M. D.; Bergman, R. G.; Raymond, K. N. *Acc. Chem. Res.* **2009**, *42*, 1650. (b) Fiedler, D.; Leung, D. H.; Bergman, R. G.; Raymond, K. N. *Acc. Chem. Res.* **2005**, *38*, 349. (c) Ulmann, P. A.; Braunschweig, A. B.; Lee, O.-S.; Wiester, M. J.; Schatz, G. C.; Mirkin, C. A. *Chem. Commun.* **2009**, 5121. (d) van Leeuwen, P. W. N. *Supramolecular Catalysis*; Wiley-VCH: Weinheim, Germany, 2008; and references cited therein.

(4) (a) Mukherjee, P. S.; Pramanik, S.; Shanmugaraju, S. In *Pt/Pd-ethynyl bond containing fluorescent molecular architectures as sensors for nitroaromatics in Molecular Self-Assembly: Advances and Applications*; Li, A. D. Q., Ed.; Pan Stanford Publishing: Singapore, 2013; pp 259−299. (b) Steed, J. W. *Chem. Soc. Rev.* **2009**, *38*, 506. (c) Gao, J.; Riis-




DOI: 10.1021/ic502581x
*Inorg. Chem.* 2015, 54, 2543−2550

Johannessen, T.; Scopelliti, R.; Qian, X. H.; Severin, K. *Dalton Trans.* **2010**, *39*, 7114. (d) Yao, L. Y.; Qin, L.; Xie, T. Z.; Li, Y. Z.; Yu, S. Y. *Inorg. Chem.* **2011**, *50*, 6055. (e) Hargrove, A. E.; Nieto, S.; Zhang, T.; Sessler, J. L.; Anslyn, E. V. *Chem. Rev.* **2011**, *111*, 6603.
(5) (a) Yoshizawa, M.; Klosterman, J. K.; Fujita, M. *Angew. Chem., Int. Ed.* **2009**, *48*, 3418. (b) Inokuma, Y.; Kawano, M.; Fujita, M. *Nat. Chem.* **2011**, *3*, 349. (c) Murase, T.; Fujita, M. *Chem. Rec.* **2010**, *10*, 342.
(6) (a) Dinolfo, P. H.; Hupp, J. T. *Chem. Mater.* **2001**, *13*, 3113. (b) Dinolfo, P. H.; Williams, M. E.; Stern, C. L.; Hupp, J. T. *J. Am. Chem. Soc.* **2004**, *126*, 12989. (c) Mines, G. A.; Tzeng, B.-C.; Stevenson, K. J.; Li, J.; Hupp, J. T. *Angew. Chem., Int. Ed.* **2002**, *41*, 154.
(7) Dsouza, N.; Pischel, U.; Nau, W. M. *Chem. Rev.* **2011**, *111*, 7941.
(8) (a) Yang, H.-B.; Ghosh, K.; Das, N.; Stang, P. J. *Org. Lett.* **2006**, *8*, 3991. (b) Wong, M.-C. K.; Yam, V. W.-W. *Acc. Chem. Res.* **2011**, *44*, 424. (c) Tao, C.-H.; Yam, V. W.-W. *J. Photochem. Photobiol., C* **2009**, *10*, 130. (d) Li, S.; Huang, J.; Zhou, F.; Cook, T. R.; Yan, X.; Ye, Y.; Zhu, B.; Zheng, B.; Stang, P. J. *J. Am. Chem. Soc.* **2014**, *136*, 5908. (e) Shanmugaraju, S.; Jadhav, H.; Patil, Y. P.; Mukherjee, P. S. *Inorg. Chem.* **2012**, *51*, 13072. (f) Shanmugaraju, S.; Bar, A. K.; Chi, K.-W.; Mukherjee, P. S. *Organometallics* **2010**, *29*, 2971. (g) Zhang, J.; Xu, X.-D.; Chen, L.-J.; Luo, Q.; Wu, N.-W.; Wang, D.-X.; Zhao, X.-L.; Yang, H.-B. *Organometallics* **2011**, *30*, 4032. (h) Wang, W.; Yang, H.-B. *Chem. Commun.* **2014**, *50*, 5171 and references cited therein.
(9) (a) Samanta, D.; Mukherjee, P. S. *Dalton Trans.* **2013**, *42*, 16784. (b) Shanmugaraju, S.; Joshi, S. A.; Mukherjee, P. S. *Inorg. Chem.* **2011**, *50*, 11736. (c) Shanmugaraju, S.; Samanta, D.; Gole, B.; Mukherjee, P. S. *Dalton Trans.* **2011**, *40*, 12333.
(10) Chakraborty, S.; Mondal, S.; Bhowmick, S.; Ma, J.; Tan, H.; Neogi, S.; Das, N. *Dalton Trans.* **2014**, *43*, 13270.
(11) Leininger, S.; Olenyuk, B.; Stang, P. J. *Chem. Rev.* **2000**, *100*, 853.
(12) Stewart, J. J. P. *J. Mol. Model.* **2007**, *13*, 1173.
(13) Goto, H.; Heemstra, J. M.; Hill, D. J.; Moore, J. S. *Org. Lett.* **2004**, *6*, 889.
(14) *SMART*, version 5.628; *SAINT*, version 6.45a; *XPREP*; *SHELXTL*; Bruker AXS Inc.: Madison, WI, 2004.
(15) Sheldrick, G. M. *SADABS*, version 2.03; University of Göttingen: Göttingen, Germany, 2002.
(16) *SHELXS-97*: Sheldrick, G. M. *Acta Crystallogr.* **2008**, *A64*, 112.
(17) Spek, A. L. *Acta Crystallogr.* **2009**, *D65*, 148.
(18) Farrugia, L. J. *J. Appl. Crystallogr.* **1997**, *30*, 565.
(19) *WinGX*: Farrugia, L. J. *J. Appl. Crystallogr.* **1999**, *32*, 837.
(20) Torrie, G. M.; Valleau, J. P. *J. Comput. Phys.* **1997**, *23*, 187.
(21) Kumar, S.; Rosenberg, J. M.; Bouzida, D.; Swendsen, R. H.; Kollman, P. A. *J. Comput. Chem.* **1992**, *13*, 1011.
(22) Sotomayor, M.; Schulten, K. *Science* **2007**, *316*, 1144.
(23) Berendsen, H. J. C.; Postma, J. P. M.; van Gunsteren, W. F.; Hermans, J. In *Intermolecular Forces*; Pullman, B., Ed.; Reidel: Dordrecht, The Netherlands, 1981; p 1331.
(24) Bjelkmar, P.; Larsson, P.; Cuendet, M. A.; Hess, B.; Lindahl, E. *J. Chem. Theory Comput.* **2010**, *6*, 459.
(25) Hess, B.; Bekker, H.; Berendsen, H. J. C.; Fraaije, J. G. *J. Comput. Chem.* **1997**, *18*, 1463.
(26) Pronk, S.; Páll, S.; Schulz, R.; Larsson, P.; Bjelkmar, P.; Apostolov, R.; Shirts, M. R.; Smith, J. C.; Kasson, P. M.; van der Spoel, D.; Hess, B.; Lindahl, E. *Bioinformatics* **2013**, *29*, 845.


DOI: 10.1021/ic502581x
*Inorg. Chem.* 2015, 54, 2543−2550